ACS Photonics

Article

pubs.acs.org/journal/apchd5

Highly Luminescent and Optically Switchable Hybrid Material by One-Pot Encapsulation of Dyes into MgAPO-11 Unidirectional Nanopores

Virginia Martínez-Martínez,*[,†] Raquel García,*[,‡] Luis Gómez-Hortigüela,[‡] Rebeca Sola Llano,[†] Joaquín Pérez-Pariente,[‡] and Iñigo López-Arbeloa[†]

[†]Departamento de Química Física, Universidad del País Vasco, UPV/EHU, Apartado 644, 48080 Bilbao, Spain

[‡]Instituto de Catálisis y Petroleoquímica-CSIC, C/Marie Curie 2, 28049, Cantoblanco, Madrid, Spain

Supporting Information

ABSTRACT: In this work a highly fluorescent hybrid material with strong anisotropic response is obtained by "one-pot" synthesis. The system is based on the "in situ" encapsulation of two chromophores, acridine (AC) and pyronine Y (PY), with similar molecular structure but perpendicular dipole moment vectors, into the 1D-nanochannels of MgAPO-11 aluminophosphate crystals (AEL structure). This non-diffusional-limited synthetic approach allows the filling of very long channels, reducing considerably the time of sample preparation (>10 μm rectangular-like AEL particles), as well as a perfect fit between the molecular and channel dimensions, avoiding the leakage of the guest dyes and any Davidov coupling. As a consequence, both dyes are embedded only in momomeric units and preferentially aligned with their long molecular axes along the channels. Interestingly, the less bulky nature of AC without pendant groups leads to a much stronger incorporation with respect to PY (48:1), enabling an efficient FRET process between them. The final solid hybrid material shows fluorescent quantum yields higher than the respective dyes in diluted solution together with blue (AC)/green (PY) fluorescence color switching depending on the direction of the polarizers upon UV light excitation.

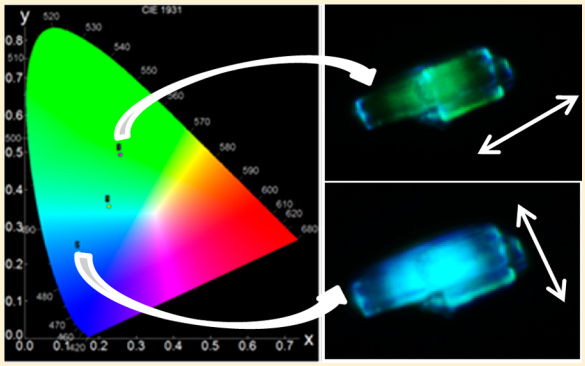

KEYWORDS: *acridine, pyronine, aluminophosphates, 1D-alignment, FRET process, high fluorescence, color switching, polarized light*

Materials with 1D-nanochannels with diameter sizes in the range of molecular dimensions are considered ideal hosts for supramolecular organization of photoactive guest molecules.[1−8] In particular, zeolite L is one of the most widely used inorganic systems to accommodate a great variety of dyes as guests.[9−11] Thus, guest−zeolite L composites can offer unique properties for the development of FRET-sensitizer solar cells, photonic wires, luminescent solar concentrators, dichroic materials, data storage devices, etc.[12−17] Many of their potential applications rely on the anisotropic arrangement of the dye molecules in a strategic way along the nanochannels to enable electronic excitation energy migration via a FRET process, mimicking antenna processes in natural photosynthesis.[18]

However, the synthesis of these hybrid materials is not trivial, and several factors have to be taken into account when considering the required properties. The channels of zeolite L are very sensitive to the molecular size of guest species. Therefore, a good fitting between the pore size and molecular structure is essential in order to avoid undesirable sandwich-like aggregates and to achieve the preferential orientation of the guests. For instance, relatively small aromatic molecules, i.e., naphthalene,[19] can form face-to-face dimers, decreasing the fluorescence, or can take different orientations with respect to the channels axis, i.e., acridine and xanthene dyes,[20,21] reducing the anisotropic response. On the other hand, larger molecules such as perylene dyes[22] are aligned completely parallel to the channels axis; however, a nonhomogeneous filling usually occurs, especially for crystals longer than 2 μm. Indeed, the "traffic jam" effect at the entrance (higher load at the end than at the crystal center) is typically observed in diffusional processes, and filling the channels completely can take a long time (several days or even weeks).[10,22] As a result, red-shifted *J*-aggregates are formed mainly at the crystals' entrance.[22−24] Note that prevention of *J*-aggregation is not an easy task since *J*-type Davidov coupling takes place between chromophores arranged in-line and in relatively short distances, a usual situation for high dye loading into 1D-systems. In this sense, L. De Cola et al.[22] have applied "molecular engineering" to control the distance between molecules, playing with different optically inert substituents covalently linked at the end of the chromophores to avoid such interactions. However, too bulky end groups will hinder or even block diffusion along the channels.[22]

Received: October 1, 2013
Published: February 6, 2014

We have recently demonstrated that applying "material engineering", that is, selecting the appropriate 1D-framework, i.e., AEL structure, whose topology and pore dimensions perfectly fit with the molecular structure of typical dyes, such as the xanthene-type pyronine Y, allows incorporation of the dyes exclusively as monomers and extraordinarily aligned with the channels, achieving not only a highly fluorescent material but also a huge anisotropic response with a dichoic ratio of 40.[25] It is worth noting that due to the adjusted fit between the molecular and channel dimensions, the incorporation of the dye can take place only by crystallization inclusion since the diffusion process is completely impeded, which interestingly avoids the leakage of the guests molecules.[18] In the present study, two "relatively small" dyes, acridine (AC) and pyronine Y (PY), with a similar molecular structure, are "one-pot" encapsulated into the AEL magnesium aluminophosphate framework type (MgAPO-11).

We selected acridine and pyronine Y as guest molecules (see Figure S1 in the Supporting Information) because PY has its transition dipole moment aligned with the molecular axis, but the dipolar moment of AC is perpendicular to the main molecular axis (Computational Study (B) in the Supporting Information). Interestingly, as AC and PY are expected to be preferentially aligned with their long molecular axes along the channels in momoneric units, their perpendicular transition dipole moment vectors will cause a complementary response to the linearly polarized light.[11,14]

The ideal situation would be that the color switching occurs upon a single irradiation of a particular wavelength (corresponding to the absorption of one of the dyes named donor), and then the energy is transferred to the other dye (named acceptor). According to Föster theory, the resonance energy transfer process (FRET) depends on many factors:[26] the distance between the donor and acceptor molecules, the extent of the spectra overlap between the fluorescence band of the donor and absorption band of the acceptor, the fluorescence quantum yield and lifetime of the donor, and finally the relative orientation between the donor and acceptor dipole transition vectors (factor κ^2). Both dyes show adequate photophysical properties for an effective FRET process, and although the angle between the transition moments is rather unfavored (practically perpendicular), an impressive FRET efficiency has been demonstrated due to the high probability of energy transfer between neighboring channels.[10,18] Therefore, the distance between both chromophores will be the key factor, which can be controlled by adjusting the dye loading, dye ratio, and dye distribution inside the channels.

In this work, we demonstrated that the relatively simple and fast crystallization inclusion method will allow the filling of large crystals, larger than several micrometers, with different dyes, both distributed in momoneric units and completely aligned through long channels. Interestingly, the less bulky nature of AC without pendant groups leads to a much stronger incorporation with respect to PY, giving a large donor to acceptor ratio, hence favoring the FRET process between them.[18] In this way, a highly fluorescent hybrid material with polarization−fluorescence (blue/green) color switching is achieved depending on the direction of the polarizers upon UV excitation light. These high-luminescent and optically switchable materials could be promising candidates for displays, color filters, light modulators, data storage, second-harmonic generation, etc.[27−34]

EXPERIMENTAL SECTION

Synthesis. The nanoporous magnesium-containing aluminophosphates (MgAPO-11) were prepared using phosphoric acid (Aldrich, 85 wt %), magnesium acetate tetrahydrate (99 wt %, Aldrich), aluminum hydroxide (Aldrich), ethylbutylamine (EBA, Aldrich), acridine (Scharlau, pure), and pyronine Y chloride (>75% purity, Across Organics) from gels with molar compositions of 0.2 MgO:1 P_2O_5:0.9 Al_2O_3:1 EBA:$(0.024 - x)$ PY:x AC:300 H_2O, where x was 0.012 and 0.024, as shown in Table 1. In a typical synthesis preparation (AC-PY/AEL sample), 1.60 g of phosphoric acid was mixed with 36.53 g of water and 0.31 g of magnesium acetate tetrahydrate. Then 0.98 g of aluminum hydroxide and 0.72 g of ethylbutylamine were added over this mixture, together with 0.0255 g of pyronine Y and 0.0149 g of acridine, to yield a gel of composition 0.2 MgO:1 P_2O_5:0.9 Al_2O_3:1 EBA:0.012 PY:0.012 AC:300 H_2O. After 1 h stirring, the resulting gel (pH ∼4) was introduced into 100 mL Teflon-lined stainless steel autoclaves, which were heated statically at 180 °C under autogenous pressure for 18 h. The solid products were recovered by filtration, exhaustively washed with ethanol and water, and dried at room temperature overnight.

Table 1. Synthesis Parameters of the Samples Discussed in This Work[a]

expt	x	mmol AC/100 g	mmol PY/100 g
AC/AEL	0.024	1.79	0
AC-PY/AEL	0.012	1.33	0.028

[a]Molar composition of synthesis gels: 0.2 MgO:1 P_2O_5:0.9 Al_2O_3:1 EBA:$(0.024 - x)$ PY:x AC:300 H_2O; amount of dye loaded in the samples expressed as mmol of dye per 100 g of product.

Characterization. X-ray powder diffraction (XRD) patterns were collected with a Panalytical X'Pro diffractometer using Cu Kα radiation. The dye content within the solid products was determined photometrically using a 2101/3101PC UV−vis Shimadzu spectrophotometer, by dissolving the composite material in 5 M hydrochloric acid and comparing with standard solutions prepared from known concentrations of the dyes.

Fluorescence images were recorded with an optical inverted microscope with epi configuration (Olympus BX51) equipped with a color CCD (DP72). Samples were excited with UV light by respective Chroma band-pass filters (350/50), and emission was collected with a Chroma cutoff filter from 400 nm. For polarized emission images, a polarizer (U-AN-360-3) was incorporated before the registration of the image in the CCD camera. Fluorescence spectra of particles at different polarized emission were recorded by a fiber coupling from Olympus to an Edinburgh Instruments spectrofluorimeter (model FLSP 920).

Fluorescence single-particle measurements were performed in a time-resolved fluorescence confocal microscope (model Micro Time 200, PicoQuant). The excitation was performed at 410 nm with a picosecond pulsed diode laser with 100 ps pulses at 5 MHz repetition rate. The fluorescence signal was collected by the same objective and focused (via a 50 μm pinhole) onto avalanche photodiode detectors (Micro-Photon-Devices MPD-APD). Decay curves recorded were fitted to exponentials, and the lifetimes were obtained from their slopes. The goodness of the fit was determined by the chi-square statistical parameter and the distribution of the residuals.

Polarization measurements were performed with unpolarized excitation light, and the emission was collected by a polarizer

dx.doi.org/10.1021/ph4000604 | ACS Photonics 2014, 1, 205−211

beam splitter that divides the signal into two mutually perpendicular polarization orientation beams and was simultaneously detected by two detector channels. We analyzed the dichroic ratio (D), defined as the relation between the emission intensity counts collected for two perpendicularly polarized radiations.

The absorption spectra of the dye/MgAPO materials were registered in powder samples in a Varian spectrophotometer (model Cary 4E), detecting the reflected light by means of an integrating sphere. The respective spectra of MgAPO crystals synthesized under identical conditions but without dyes were recorded and subtracted from the sample signal to eliminate the scattering contribution of particles to the absorption spectra. Emission spectra of the powder were recorded in a SPEX spectrofluorimeter (model Fluorolog 3-22) in front-face configuration. Absolute photoluminescence quantum yield of the dye/MgAPO-11 powder was measured in an integrated sphere (Horiba Scientific, model Quanta-phi) coupled to the spectrofluorimeter.

The AEL AlPO framework with occluded PY and AC molecules (AC-PY/AEL) was studied by density functional theory, using atomic orbitals as numerical basis set, as implemented in the DMol3 module[35] in the Material Studio software package.[36] Calculations were performed under periodic boundary conditions (PBC), using a DNP basis set and the PBE generalized gradient approximation as exchange–correlation functional;[37] dispersion interactions were accounted for through the Grimme dispersion method (DFT+D).[38] Supercells of 1 × 1 × 3 unit cells along the channel direction were built with one organic dye included as monomer, and the systems were geometry-optimized. AC was studied in its protonated form, as determined from the experimental results. Molecular volumes were obtained from Connolly surfaces, using a radius of 1.0 Å.

RESULTS AND DISCUSSION

In our previous work, we showed that the Mg-containing nanoporous aluminophosphate MgAPO-11 (AEL-type structure) represents an optimal host for the encapsulation of a xanthene-type dye, pyronine Y.[25] MgAPO-11 possesses a one-dimensional system of 10-ring elliptical channels with dimensions (6.5 × 4 Å) close to those of the PY molecule and with a particular channel topology that contains pockets along the channel direction (Figure S1 in the Supporting Information). These two factors cause the unique incorporation of monomeric units of PY in the channel system, leading to a hybrid material with high green emission efficiency and an extraordinarily preferential alignment of the dye molecules along the channels.

On the other hand, acridine possesses a similar molecular structure to xanthene-type dyes, consisting in three fused aromatic rings, though with one nitrogen in the central ring and no lateral pendant groups. An important characteristic of AC is that it presents its absorption/emission transition moment vector along the short molecular axis (see Computational Study (B) in the Supporting Information), being perpendicular to that of PY. However, due to the geometric constraints imposed by the 1D-nanochannels, both dyes are expected to be incorporated with preferred alignment of their main molecular axis roughly parallel to the channel direction, giving a complementary response to the linear polarized light.

First, AC was incorporated into the nanochannels of MgAPO-11 as the unique dye by the crystallization inclusion method, following a similar procedure to that described previously for PY dye.[25] Ethylbutylamine was used as the organic structure directing agent (SDA), and AC was added to the synthesis gel in a molar ratio of 0.024 AC/1 P_2O_5 (Table 1), yielding pure MgAPO-11 (Figure 1).

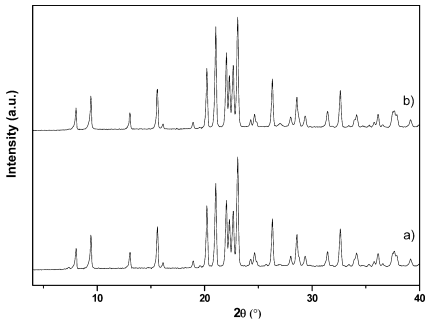

Figure 1. X-ray diffraction pattern of (a) AC/AEL; (b) AC-PY/AEL.

The amount of AC incorporated in the product was around 50 times higher than that of the material containing PY as the only dye;[25] this is ascribed to the smaller size and higher solubility in the synthesis gel of AC.

Indeed, computational results show a much better quality of the interactions (normalized to the molecular size, i.e., interaction per non-H atom or per molecular volume unit; see Table 2), and therefore a better fit, of AC with the AEL framework channels compared to those of PY (Figure 2); the molecular structure and dimensions of AC and PY and the AEL channels are displayed in Figure S1 (Supporting Information), where the much higher dimensions of PY, especially in the shortest molecular axis, which is the one that is more restricted with respect to the AEL channel size, are shown. Due to the higher number of atoms of PY, the overall interaction energy per molecule is slightly higher for PY than for AC (Table 2). However, when the results are normalized to interaction energy per non-H atom (C + N + O) or per molecular volume unit (Å^3), which represents a better estimation of the quality of the intermolecular AEL–dye interactions (i.e., fitting), taking into account the space-filling effect (it should be considered that the void space left by the dye will be filled by the SDA molecules), we observe that the quality of the interactions is much higher for AC, evidencing a much better adjustment of its molecular dimensions with those of the AEL channels. These energy results explain the much higher incorporation of AC dyes found experimentally.

Table 2. Molecular Volumes of AC and PY Dyes, Interaction Energies (Expressed in Different Forms, in kcal/mol), and Tilting Angles of the Dyes Incorporated within the AEL Framework

		interaction energy (in kcal/mol)			
dye	molecular volume (Å^3)	per molecule	per non-H atom	per volume (Å^3)	tilting angle
AC	167.2	−232.1	−16.6	−1.38	9
PY	276.7	−240.1	−12.0	−0.87	0

The transmission image of AC/AEL crystals of several micrometers with rectangular shape displays a slight pale yellow color, and the respective fluorescence image shows a cyan-blue emission color, characteristic of AC, under UV illumination

dx.doi.org/10.1021/ph4000604 | ACS Photonics 2014, 1, 205–211

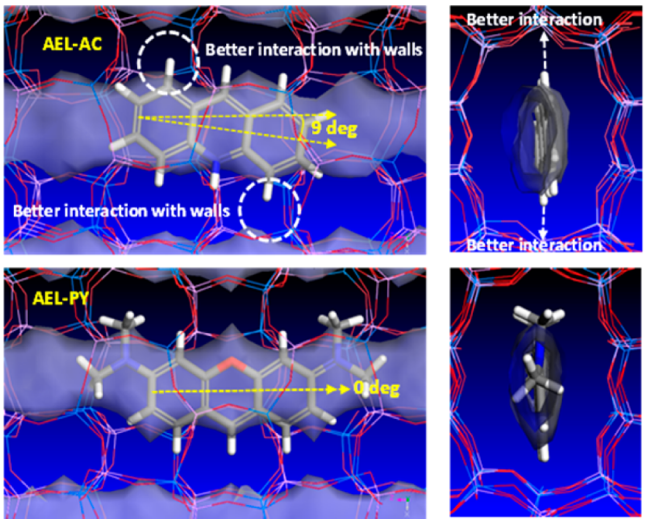

Figure 2. AC (top) and PY (bottom) confined within the AEL channels, and deviation angles; the channel void volume is shown to help with interpretation.

(Figure 3). To spectroscopically characterize the AC dye within the AEL structure, measurements were performed in bulk

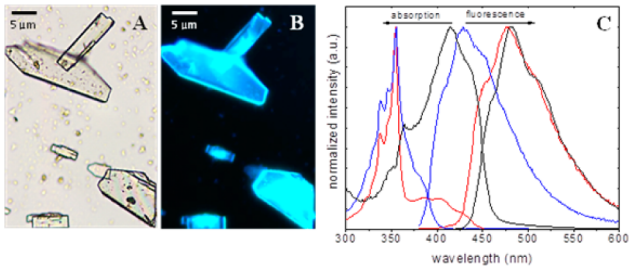

Figure 3. (Left) Transmission (A) and fluorescence (B) images under UV illumination (350/50) of AC/AEL crystals. (Right) (C) Absorption and fluorescence spectra of acridine dye in aqueous solution (10^{-5} M) at different pHs (red curve: pH < pK_a, blue curve: pH > pK_a) and bulk powder of AC/AEL (black curve).

powder and single AC/AEL crystals. The main absorption band for the AC/AEL powder sample is centered at 414 nm (Table 3, Figure 3), which corresponds to the S_0–S_1 electronic

Table 3. Main Photophysical Parameters of AC/AEL, PY/AEL, and AC-PY/AEL

sample	λ_{abs}/nm	λ_{flu}/nm	τ_{flu}/ns(A%)	ϕ_{fl}	D
PY/AEL[a]	523	536	3	0.21	40
AC/AEL	414	481	27	0.54	5[b]
AC:PY/AEL	413/525	480/537	7(30)/23(70)	0.26	

[a]Taken from ref 25. [b]Corresponds to "1/D" value.

transition calculated for the isolated protonated form of AC dye (ACH^+) (Computational Study (B) in the Supporting Information). However, its intensity considerably increases with respect to the typical, more intense S_0–S_2 in UV, located at 354 nm, recorded for AC in aqueous solution (Table S2 and Computational Study (B) in the Supporting Information). A less prominent change in the intensity ratio between these transitions has been previously observed for methylacridine dye inside zeolite L channels and was attributed to the change from isotropic liquid media to the zeolitic phase.[21] Additionally, note that the absorption band at around 415 nm is predicted only for the protonated form of AC dye (ACH^+) and experimentally is registered as a shoulder in AC solutions at pH < pK_a (pK_a = 5.6).[39] Besides, the AC/AEL sample (measurements in powder or single particle) shows an emission band located at around 481 nm, analogous to that recorded in acid aqueous solution (Table 3 and Figure 3).

Moreover, fluorescence lifetime curves registered in AC/AEL (Table 3) show, in contrast to the biexponential decay functions for AC dye in solution (representative of the neutral and protonated forms in equilibrium, with lifetimes of 8 and 30 ns, respectively, whose proportions depend on the pH; see Table S2 in the Supporting Information), a clear monoexponential kinetics with a fluorescence lifetime of 27 ns (for powder sample and single-crystal sample, Figure S2 in the Supporting Information). All these spectroscopic features indicate that the AC dye is incorporated within the AEL framework mainly in its protonated form (ACH^+).

It is worth remarking that the encapsulation of AC dye within the AEL structure produces an increase of its absolute quantum yield (ϕ_{fl} = 0.54, Table 3) with respect to that of AC solution (ϕ_{fl} = 0.41 at pH < 5.6 or 0.32 at pH > 5.6, Table S2 in the Supporting Information). Not only does the host matrix, AEL, enable the encapsulation of only AC monomers in a more rigid configuration but also, particularly for this dye, the encapsulation method and nature of the AEL channels favor its protonated form, whose quantum yield is higher than the respective neutral form.

The total suppression of dye aggregation even for less bulkier dyes without pendant groups, such as AC, makes the AEL framework an ideal host for the encapsulation of dyes with a relatively small molecular structure with three fused rings. The crystallization inclusion method could be successfully applied for many other typical dyes with a similar molecular structure such as acridines, xanthenes, oxacines, and thionines.[39] This synthetic "one-pot" approach enables the filling of large crystals (long AEL channels), avoiding the "traffic jam" effect at the entrance and reducing considerably the sample preparation time (less than 24 h) with respect to a diffusional process,[40] especially for particles larger than several micrometers (where several days or weeks are required). In addition, the leakage of the dye guests out of the channels is impeded by their tight fit with the matrix and by the presence of the SDA molecules, avoiding the need for closing the channel openings.

Fluorescence dichroic ratios "D", defined as the ratio between the emission signal for polarized light parallel and perpendicular to the channel directions, in AC/AEL single crystals are determined by confocal fluorescence microscopy to gain information on the alignment of AC molecules (Figure S2 in the Supporting Information). Note that an inverse anisotropic response to the polarized detection is expected for AC dye in AEL single crystals; that is, higher emission intensity is expected to be collected for the perpendicularly polarized direction to the c-axis of AEL nanochannels with respect to the parallel one, due to the disposition of its transition dipole moment of the S_1–S_0 transition along the short molecular axis (see Computational Study (B) in the Supporting Information). Thus, in this case "1/D" values of around 5–5.5 indicate a preferential orientation of AC molecules into the internal 1D-pores (Table 3). Computational results show indeed that AC molecules are not perfectly aligned with the channel direction, but are slightly tilted with an angle

dx.doi.org/10.1021/ph4000604 | ACS Photonics 2014, 1, 205–211

of 9 deg in order to optimize the interaction with the channel walls in both molecular sides (see Figure 2). In contrast, the larger dimensions of PY force the molecule to perfectly align with the channel direction, with the bulky methyl groups of PY sited on the AEL side-pockets, explaining its much higher dichroic ratio (≥40) observed experimentally.[25]

In the next step, in order to achieve fluorescence color switching by linear polarized light, in a similar fashion to other dye-loaded zeolite L systems,[11,14] the co-encapsulation of AC and PY dyes within the MgAPO-11 structure was performed by crystallization inclusion with an equimolar ratio of both dyes in the initial gel (AC-PY/AEL in Table 1). It is worth noting that although a much higher amount of AC dye is taken up by the solid product, around 48 times higher than PY (Table 1) because of its better fit (Table 2), the intensity of the emission band of each dye, centered at 480 and 537 nm for AC and PY, respectively, is very similar under UV excitation (Figure 4, left).

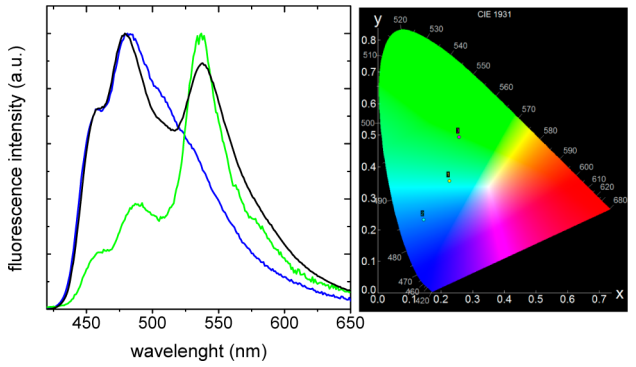

Figure 4. (Left) Emission spectra for a AC-PY/AEL single particle (black) without polarization and for perpendicular (blue) and parallel (green) polarizations to the *c* channel axis of MgAPO-11 (under UV excitation, 350/50). (Right) Their corresponding emission colors in CIE with coordinates $x = 0.23$ and $y = 0.35$ (black emission curve); $x = 0.15$ and $y = 0.23$ (blue emission curve); $x = 0.26$ and $y = 0.49$ (green emission curve), respectively.

The AC-PY/AEL sample shows a whitish-cyan emission with a relatively high fluorescence efficiency ($\phi_{fl} = 0.26$, Table 3), which corresponds in the CIE chromaticity diagram (mathematical definition of color spaces by the International Commission on Illumination, 1931) to coordinates $x = 0.23$ and $y = 0.35$, not far from the definition of white light ($x = y = 0.33$).

This observed fact is attributed to a rather efficient energy transfer (FRET) from AC (donor) to PY (acceptor), which are distributed close enough to enable coupling of their electronic transition dipole moments. Note that a Föster ratio (R_0 defined as the distance at which the FRET is 50% efficient) of around 23−25 Å is calculated, assuming a refraction index, η, between 1.4 and 1.55 and an orientation factor $\kappa^2 \approx 0.1$, quite unfavored for the hetero-FRET process along the channel.

In this regard, considering the dye contents for AC-PY/AEL (Table 1) and the dimensions of the AEL unit cell along the channel (8.37 Å), and assuming a homogeneous distribution of the dyes along single channels, there is one molecule of AC every 516 Å and one molecule of PY dye every 24502 Å along a particular channel. This result indicates that the probability of finding a PY and an AC molecule in the same channel in that distance interval is rather small (4% and 12% for distances below 20 and 60 Å, respectively, for each PY), unless there is a clustering of dyes within single channels, which does not seem to be the case from our observations. As a consequence, the FRET process must preferentially take place between dye molecules located in different channels.

The probability of finding an AC molecule around a given PY in neighboring channels at a distance below 20 or 60 Å is rather high (20% and 100%, respectively), despite the low content of dyes, due to the high number of neighboring channels (see Figure S3 in the Supporting Information), as other authors have also stated.[10,18] The decreasing of the lifetime of AC from 27 to 23 ns, Table 3, is a direct consequence of the radiationless energy transfer process to PY. Indeed, the relatively high fluorescence efficiency and long lifetimes of emission of the donor (AC) together with the relatively high overlapping between its emission band and the absorption band of the acceptor (PY, see S4 in the Supporting Information, gray area) are favorable factors for FRET.[26] Moreover, as other authors have proposed, relatively large donor:acceptor ratios (i.e., 50:1) are preferred for an efficient FRET process,[18] in concordance with the relative contents of the dyes determined in our work (48:1). In addition to this hetero-FRET process between PY and AC, an energy migration between AC molecules (homo-FRET process) in neighboring channels must also be taken into account due to the relatively high AC loading (which implies shorter distances between AC molecules) and the overlapping between the absorption and emission spectra in AC (Figure S4), together with a more favored orientation factor ($\kappa^2 = 1$) for parallel transition dipoles. This involves the excitation energy collected by one AC molecule first migrating to other AC molecules (homo-FRET) and then being transferred to other PY molecules (hetero-FRET) along the 1D-channels.

One of the most important features of our AC-PY/AEL material is that, under UV excitation (corresponding to the absorption of AC), it displays blue or green emission depending on the direction of the polarizers before detection. Figure 5

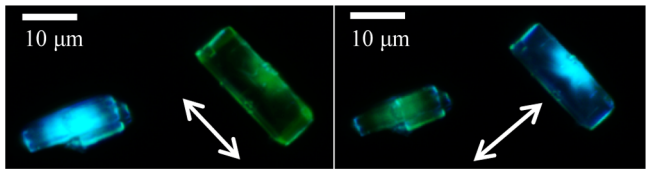

Figure 5. Transmission and polarized intensity fluorescence images of a single particle of AC-PY/AEL for orthogonal polarizations (arrows indicate the direction of the polarized light).

clearly shows the fluorescence blue-green color switching for perpendicular polarization directions before the detector. The emission spectra recorded at each polarization, that is, for the analyzer in parallel (green emission) or perpendicular (blue emission) direction with respect to the main channel direction of the AEL framework, were collected in single crystals (Figure 5).

The characteristic blue fluorescence band centered at 481 nm is observed for perpendicular polarization to the *c*-axis channels of AEL, and the typical green emission band of PY monomers into AEL channels, located at 537 nm, with a small contribution of AC dye emission, is obsesrved for the analyzer in a parallel direction to the channels.

Note that similar color switching found in solid systems for orthogonally polarized emission light is based on generation of oxidized photoproducts upon UV irradiation.[41] Remarkably, the emission switching demonstrated in our AC-PY/AEL

dx.doi.org/10.1021/ph4000604 | ACS Photonics 2014, 1, 205−211

hybrid system together with other dye−zeolite L samples[11,14] is an instantaneous and efficient process, completely reversible and reproducible. Moreover, because the switching does not involve any chemical transformation, the material will present a high fatigue resistance. All these properties are fundamental requirements for practical use as a dichroic material. Indeed, although the photoactive units are organic molecules that can suffer degradations with aging, the inorganic nature of the aluminophosphate matrix will protect them from photo- and thermodegradation.

CONCLUSIONS

The 1D-AEL framework has demonstrated to be an optimal host for the encapsulation of relatively small dyes with a general structure of three fused rings with heteroatoms, i.e., AC and PY. The resultant dye−AEL hybrid material shows high fluorescence efficiency (dye aggregation completely suppressed) and large anisotropic response (dye preferentially aligned along the channels), interesting for technological applications such as solid-state dye laser and many nonlinear optics applications.

The non-diffusional-limited crystallization inclusion method is a fast and easy "one-pot" approach that enables, in less than 24 h, the (co)-encapsulation of such kinds of dyes along the narrow AEL channels (large rectangular particles >10 μm), avoiding at the same time potential leakage of these guests.

The alignment of AC and PY dyes (with transition dipole moment vectors practically perpendicular to each other) into the 1D-nanochannels occluded at an adequate loading and ratio enables a FRET process between both dyes, hence yielding an interesting system with polarization−fluorescence switching under UV excitation.

The blue-green color tuning realized is an instantaneous and efficient process, completely reversible and reproducible with a high fatigue resistance, essential for its use in many dichroic applications.

ASSOCIATED CONTENT

Supporting Information

AC and PY molecular structures, AEL framework structure, quantum mechanics calculations on AC (Gaussian 09), photophysical parameters of AC (at different pHs) and PY dye in aqueous solution and their respective absorption and fluorescence spectra, FLIM and polarized intensity fluorescence images of AC/MgAPO-11 single crystal, calculation of the probability of finding an AC molecule around a given PY molecule at a given (R) distance. This material is available free of charge via the Internet at http://pubs.acs.org.

AUTHOR INFORMATION

Corresponding Authors

*E-mail: Virginia.martinez@ehu.es.
*E-mail: (R. García) rgs@icp.csic.es.

Author Contributions

The manuscript was written through contributions of all authors. All authors have given approval to the final version of the manuscript.

Notes

The authors declare no competing financial interest.

ACKNOWLEDGMENTS

This work was funded by the Spanish Ministerio de Economía y Competitividad (MAT2012-31127/MAT2010-20646-C04-04) and the European Research Council, under the Marie Curie Career Integration Grant program (FP7-PEOPLE-2011-CIG), Grant Agreement PCIG09-GA-2011-291877. V.M.M. and L.G.H. acknowledge Ministerio de Economía y Competitividad for Ramón y Cajal contracts (RYC-2011-09505 and RYC-2012-11794, respectively), and R.S.L. acknowledges Universidad del País Vasco (UPV-EHU) for a predoctoral fellowship. Accelrys is acknowledged for providing software, and Centro Técnico de Informática-CSIC for running the calculations. C. Márquez-Álvarez is acknowledged for his help in the calculation of probabilities.

REFERENCES

(1) Yu, J.; Cui, Y.; Wu, C.; Yang, Y.; Wang, Z.; O'Keeffe, M.; Chen, B.; Qian, G. Second-order nonlinear optical activity induced by ordered dipolar chromophores confined in the pores of an anionic metal-organic framework. *Angew. Chem., Int. Ed.* **2012**, *51*, 10542−10545.

(2) Schulz-Ekloff, G.; Wöhrle, D.; van Duffel, B.; Schoonheydt, R. A. Chromophores in porous silicas and minerals: preparation and optical properties. *Microporous Mesoporous Mater.* **2002**, *51*, 91−138.

(3) Kim, H. S.; Pham, T. C. T.; Yoon, K. B. A novel class of nonlinear optical materials based on host-guest composites: zeolites as inorganic crystalline hosts. *Chem. Commun.* **2012**, *48*, 4659−4673.

(4) Marlow, F.; Wubbenhorst, M.; Caro, J. Pyroelectric effects on molecular sieve crystals loaded with dipole molecules. *J. Phys. Chem.* **1994**, *98*, 12315−12319.

(5) Gao, F.; Zhu, G.; Chen, Y.; Qiu, S. Assembly of p-nitroaniline molecule in the channel of zeolite MFI large single crystal for NLO material. *J. Phys. Chem. B* **2004**, *108*, 3426−3430.

(6) Pham, T. C. T.; Kim, H. S.; Yoon, K. B. Growth of uniformly oriented silica MFI and BEA zeolite films on substrates. *Science* **2011**, *334*, 1533−1538.

(7) Roeffaers, M. B. J.; Ameloot, R.; Baruah, M.; Uji-i, H.; Bulut, M.; De Cremer, G.; Müller, U.; Jacobs, P. A.; Hofkens, J.; Sels, B. F.; De Vos, D. E. Morphology of large ZSM-5 crystals unraveled by fluorescence microscopy. *J. Am. Chem. Soc.* **2008**, *130*, 5763−5772.

(8) Moissette, A.; Lobo, R. F.; Vezin, H.; Bremard, C. Influence of gallium isomorphous substitution in the acidic MFI zeolite framework on the hole formation, transfer, and trapping upon incorporation of anthracene. *J. Phys Chem. C* **2011**, *115*, 6635−6643.

(9) Brühwiler, D.; Calzaferri, G. Molecular sieves as host materials for supramolecular organization. *Microporous Mesoporous Mater.* **2004**, *72*, 1−23.

(10) Calzaferri, G. Nanochannels: hosts for the supramolecular organization of molecules and complexes. *Langmuir* **2012**, *28*, 6216−6231.

(11) Bruehwiler, D.; Calzaferri, G.; Torres, T.; Ramm, J. H.; Gartmann, N.; Dieu, L-Q; Lopez-Duarte, I.; Martinez-Diaz, M. V. Nanochannels for supramolecular organization of luminescent guests. *J. Mater. Chem.* **2009**, *19*, 8040−8067.

(12) Calzaferri, G.; Maas, H.; Pauchard, M.; Pfenniger, M.; Megelski, S.; Devaux, A. Supramolecularly organized luminescent dye molecules in the channel of zeolite L. *Adv. Photochem.* **2002**, *27*, 1−50.

(13) Mahato, R. N.; Lülf, H.; Siekman, M. H.; Kersten, S. P.; Bobbert, P. A.; de Jong, M. P.; De Cola, L.; van der Wiel, W. G Ultrahigh magnetoresistance at room temperature in molecular wires. *Science* **2013**, *341*, 257−260.

(14) Cucinotta, F.; Popovic, Z.; Weiss, E. A.; Whitesides, G. M.; De Cola, L. Microcontact transfer printing of zeolite monolayers. *Adv. Mater.* **2009**, *21*, 1142−1145.

(15) Li, Z.; Luppi, G.; Geiger, A.; Josel, H.-P.; De Cola, L. Bioconjugated fluorescent zeolite L nanocrystals as labels in protein microarrays. *Small* **2011**, *7*, 3193−3201.

(16) Bruhwiler, D.; Dieu, L-Q; Calzaferri, G. Nanochannel materials for quantum solar energy conversion devices. *Chimia* **2007**, *61*, 820−822.

(17) Bruhwiler, D.; Kunzmann, A.; Calzaferri, G. ZeoFRET nanochannel-materials for solar energy conversion devices. *EPA Newsletter* **2011**, 25−27.
(18) Calzaferri, G.; Meallet-Renault, R.; Bruhwiler, D.; Pansu, R.; Dolamic, I.; Dienel, T.; Adler, P.; Li, H.-R.; Kunzmann, A. Designing dye-nanochannel antenna hybrid materials for light harvesting, transport and trapping. *ChemPhysChem* **2011**, *12*, 580−594.
(19) Hashimoto, S.; Hagiri, M.; Matsubara, N.; Tobitab, S. Photophysical studies of neutral aromatic species confined in zeolite L: comparison with cationic dyes. *Phys. Chem. Chem. Phys.* **2001**, *3*, 5043−5051.
(20) Fois, E.; Tabacchi, G.; Calzaferri, G. Orientation and order of xanthenes dyes in the one-dimensional channels of zeolite L: bridging the gap between experimental data and molecular behavior. *J. Phys. Chem. C* **2012**, *116*, 16784−16799.
(21) Fois, E.; Tabacchi, G.; Devaux, A.; Belser, P.; Brühwiler, D.; Calzaferri, G. Host-guest interactions and orientation of dyes in the one-dimensional channels of zeolite L. *Langmuir* **2013**, *29*, 9188−9198.
(22) Busby, M.; Devaux, A.; Blum, C.; Subramaniam, V.; Calzaferri, G.; De Cola, L. Interactions of perylene bisimide in the one-dimensional channels of zeolite L. *J. Phys. Chem. C* **2011**, *115*, 5974−5988.
(23) Gartzia-Rivero, L.; Bañuelos-Prieto, J.; Martínez-Martínez, V.; López-Arbeloa, I. Versatile photoactive materials based on zeolite L doped with laser dyes. *ChemPlusChem* **2012**, *77*, 61−70.
(24) Busby, M.; Blum, C.; Tibben, M.; Fibikar, S.; Calzaferri, G.; Subramaniam, V.; De Cola, L. Time, space, and spectrally resolved studies on J-aggregate interactions in zeolite L nanochannels. *J. Am. Chem. Soc.* **2008**, *130*, 10970−10976.
(25) Martínez-Martínez, V.; García, R.; Gómez-Hortigüela, L.; Pérez-Pariente, J.; López-Arbeloa, I. Modulating dye aggregation by incorporation into 1D-MgAPO nanochannels. *Chem.—Eur. J.* **2013**, *19*, 9859−9865.
(26) Lakowicz, J. R. *Principles of Fluorescence Spectroscopy*, 3rd ed.; Springer: New York, 2006.
(27) Zhu, R.; Kumar, A.; Yang, Y. Polarizing organic photovoltaics. *Adv. Mater.* **2011**, *23*, 4193−4198.
(28) Kocher, C.; Weder, C.; Smith, P. Dichroic ultraviolet light filters. *Appl. Opt.* **2003**, *42*, 5684−5692.
(29) Montali, A.; Bastiaansen, C.; Smith, P.; Weder, C. Polarizing energy transfer in photoluminescent materials for display applications. *Nature* **1998**, *392*, 261−264.
(30) Yelleswarapu, C. S.; Rao, D. V. G. L. N. Photonic applications with photoanisotropic nanomaterials. *Opt. Spectrosc.* **2011**, *111*, 208−214.
(31) Hu, D.-Q.; Zhang, Z.-S.; Hu, Y.-L.; Luo, Y.-H.; Zhang, Q.-J.; Huang, W.-H. Study on the rewritability of bisazobenzene-containing films in optical storage based on two-photon process. *Opt. Commun.* **2010**, *284*, 802−806.
(32) Kendhale, A. M.; Schenning, A. P. H. J.; Debije, M. G. Superior alignment of multi-chromophoric perylenebisimides in nematic liquid crystals and their application in switchable optical waveguides. *J. Mater. Chem. A* **2013**, *1*, 229−232.
(33) Yun, C.; You, J.; Kim, J.; Huh, J.; Kim, E. Photochromic fluorescence aswitching from diarylethenes and its applications. *J. Photochem. Photobiol. C* **2009**, *10*, 111−129.
(34) Salamonczyk, M.; Kovarova, A.; Svoboda, J.; Pociecha, D.; Gorecka, E. Switchable fluorescent liquid crystals. *App. Phys. Lett.* **2009**, *95*, 171901-1−171901-3.
(35) Delley, B. From molecules to solids with the DMol3 approach. *J. Chem. Phys.* **2000**, *113*, 7756−7764.
(36) *DMol3Module, Materials Studio 6.0*; Accelrys, Inc.: San Diego, CA, 2010.
(37) Perdew, J. P.; Burke, K.; Ernzerhof, M. Generalized gradient approximation made simple. *Phys. Rev. Lett.* **1996**, *77*, 3865−3868.
(38) Grimme, S. J. Semiempirical GGA-type density functional constructed with a long-range dispersion correction. *Comput. Chem.* **2006**, *27*, 1787−1799.
(39) Brown, H. C.; Baude, E. A.; Nachod, F. C. *Determination of Organic Structures by Physical Methods*; Academic Press: New York, 1955.
(40) Martínez-Martínez, V.; García, R.; Gómez-Hortigüela, L.; Pérez-Pariente, J.; López-Arbeloa, I. Material fotoactivo, método de obtención y uso del material, Spanish Patent P201231259, 2012.
(41) Houjou, H.; Takezawa, S.; Oyamada, I.; Matsumura, K.; Seino, H.; Yoshikawa, I.; Mizobe, Y.; Araki, K. Blue/red linear dichroic emission from a highly anisotropic crystal of triarylmethane dye conjugated with phenoxo-zinc complexes. *Chem.—Eur. J.* **2011**, *17*, 1122−1127.